

Chapter 5
**Characterisation of neurochemically distinct populations of
colonic viscerofugal neurons**

INTRODUCTION

In the guinea pig intestine, all viscerofugal neurons traced from the coeliac and inferior mesenteric ganglia have been reported to contain ChAT (Mann et al., 1995, Sharkey et al., 1998). Of these, about 60-70% of viscerofugal neurons in the large intestine, but none in the small intestine, also contain immunoreactivity for nitric oxide synthase (NOS+; Anderson et al., 1995, Mann et al., 1995). The population of NOS+ viscerofugal neurons may be a subclass of viscerofugal neurons, present in the large intestine but not in the small intestine. A possible functional role of NOS+ viscerofugal neurons may be activation of secretomotor reflexes, since NOS+ varicosities from the intestine preferentially surround secretomotor sympathetic neurons in the coeliac ganglion (Costa and Furness, 1984, Anderson et al., 1995).

Estimates of the proportions of enteric viscerofugal neurons that contain specific substances have been made by sampling from populations that project to a particular target; usually prevertebral ganglia. However, viscerofugal neurons in a particular gut region can also be labelled from extrinsic nerve trunks, close to the gut. In this case, the proportions of viscerofugal neurons that contain specific substances may accurately reflect the entire population of viscerofugal neurons in that region, rather than only those which project to a specific target ganglion that has been injected with a tracer. In the distal colon, these populations may include viscerofugal neurons to the coeliac ganglia (Messenger and Furness, 1992), superior mesenteric ganglia (Messenger and Furness, 1993), inferior mesenteric ganglia (Messenger and Furness, 1993), pelvic ganglia (Luckensmeyer and Keast, 1995a), or the spinal cord (Neuhuber et al., 1993, Suckow and Caudle, 2008). Rapid neuronal tracing from

extrinsic nerve trunks in vitro has been applied using biotinamide (Tassicker et al., 1999a). Biotinamide tracing can reveal the fine morphological details of viscerofugal neuron cell bodies (Tassicker et al., 1999a). Previous studies extensively utilized Fast Blue for retrograde tracing from prevertebral ganglia, which successfully identifies viscerofugal neuron cell bodies (Kuramoto and Furness, 1989, Furness et al., 1990c, Messenger and Furness, 1992, Barbiers et al., 1993, Messenger and Furness, 1993, Anderson et al., 1995, Luckensmeyer and Keast, 1995a, 1996, Karila et al., 1997, Li and Masuko, 1997, Sharkey et al., 1998, Furness et al., 2000b, Lomax et al., 2000). However, the morphological detail of neuronal processes may not always be completely revealed (Kuramoto and Furness, 1989). In this study, we aimed to characterize the populations of viscerofugal neurons in the distal colon using combined immunohistochemistry for ChAT and NOS, with rapid neuronal tracing from extrinsic nerves in vitro, using biotinamide.

METHODS

Dissection

Adult guinea pigs, weighing 200-350g, were euthanized by stunning and exsanguination as approved by the Animal Welfare Committee of Flinders University. Segments of distal colon (>20mm from the anus) and attached mesentery were removed and immediately placed into a Sylgard-lined petri dish (Dow Corning, Midland, MI) filled with oxygenated Krebs solution at room temperature. Krebs solution contained (mM): NaCl 118; KCl 4.7, NaH₂PO₄·2H₂O 1; NaHCO₃ 25; MgCl₂·6H₂O 1.2; D-Glucose 11; CaCl₂·2H₂O 2.5; bubbled with 95%O₂ and 5%CO₂. Segments were cut open along the mesenteric border and pinned flat with the mucosa uppermost. The mucosa and submucosa were removed by sharp dissection. Single extrinsic nerve trunks (3-10mm long) were dissected free from surrounding mesentery.

Biotinamide labelling

Dissected preparations (8-20mm in length) were transferred and pinned into a partitioned Sylgard-lined dish. The nerve trunk ran under a glass coverslip and was pinned in a small Perspex isolation chamber sealed with high-vacuum silicon grease (Ajax, Auburn, NSW Australia). A bubble of biotinamide solution (5% biotinamide (N-[2-aminoethyl] biotinamide hydrobromide), dissolved in artificial intracellular solution (150 mmol/L monopotassium L-glutamic acid, 7 mmol/L MgCl₂, 5 mmol/L glucose, 1 mmol/L ethylene glycolbis(β-aminoethyl ether)-N,N,N=N-tetraacetic acid, 20 mmol/L HEPES buffer, 5 mmol/L disodium adenosine triphosphate, 0.02% saponin, 1% dimethyl sulfoxide, 100 IU/mL penicillin, 100 µg/mL streptomycin, and

20g/mL gentamycin sulphate) was placed on the dissected nerve trunk and normal Krebs solution in the main chamber was replaced with sterile culture medium (Dulbecco's modified Eagle's [DME]/Han's F12, Sigma [1:1 ratio mix, supplemented with L-glutamine and 15 mM HEPES]; including 10% fetal bovine serum (Gibco, Life Technologies Corporation, USA), 100 IU/ml penicillin (Pen Strep, Gibco), 100 µg/ml streptomycin D (Pen Strep, Gibco), 10 µg/ml gentamycin (Gibco), 2.5 µg/ml amphotericin B (Sigma), and 1.8 mM CaCl₂ (Tassicker et al., 1999). After 16 hours, preparations were maximally stretched and fixed in modified Zamboni's fixative (2% formaldehyde, 0.2% saturated picric acid in 0.1M phosphate buffer, pH 7.0) for approximately 24 hours at 4°C. Tissue was then cleared with three washes of 100% dimethylsulphoxide (DMSO), and stored in PBS at 4°C.

Immunohistochemistry

Cleared preparations were incubated with antisera to choline acetyltransferase (1:1,000) and nitric oxide synthase (1:1,000) at room temperature for two days. Preparations were rinsed three times in PBS and incubated with secondary antisera for 4 hours at room temperature. Biotinamide was labelled with streptavidin conjugated to Alexa488 (dilution 1:2,000; Molecular Probes). After a final rinse with PBS, preparations were equilibrated with 50%, 70%, and 100% carbonate-buffered glycerol, and mounted on glass slides in 100% carbonate-buffered glycerol (pH 8.6). All antibodies were diluted in 0.1 M PBS (0.3 M NaCl) containing 0.1% sodium azide. Controls for double-labelling were performed by omitting one or more primary antibodies from the procedure, and by ensuring that all combinations of primary and secondary antisera were free of cross-reactivity.

Antibodies

ChAT antibodies were raised in rabbit and generously provided by Dr. M. Schemann of Technische Universität München, code: P3YEB. The immunizing antigen was a 22 amino acid peptide fragment of purified porcine ChAT (GLFSSYRLPGHTQDTLVAQKSS; amino acids 168-189). Neuronal NOS antibodies were raised in sheep and generously provided by Dr. P.C. Emson (Babraham Institute, Molecular biology, Cambridge), code: K205. The immunizing antigen was recombinant rat neuronal NOS. Both antibodies are polyclonal and have been characterized in western blots of guinea pig inferior mesenteric ganglia and pelvic ganglia (Olsson et al., 2006). Secondary antibodies were donkey anti-sheep immunoglobulin G conjugated to indodicarbocyanine Cy5 (Jackson, cat. no. 713-175-147, dilution 1:100) and donkey anti-rabbit immunoglobulin G conjugated to indodicarbocyanine (CY3; Jackson, cat. no. 711-165-152; dilution 1:400).

Microscopy, image analysis and processing

Specimens were examined on an Olympus IX71 microscope (Olympus Corporation, Japan) equipped with epifluorescence and highly discriminating filters (Chroma Technology Co., Battledore, VT). Images were captured using a Roper scientific (Coolsnap) camera at 1392 x 1080 pixels, using AnalySIS Imager 5.0 (Olympus-SIS, Münster, Germany) and saved as TIFF files. Matched micrographs of immunohistochemically-labelled nerve structures were captured using a 40x objective water-immersion lens. All biotinamide-labelled cell bodies were sampled and tested for immunoreactivity for choline acetyltransferase (ChAT) and nitric oxide synthase (NOS). All cell bodies classified as ChAT- or NOS-immunoreactive (IR) were present in micrographs where all pixels less than or equal to three standard

deviations above the mean value of background fluorescence had been removed. Biotinamide-labelled cell bodies were excluded from the sample when they were overlying another biotinamide-labelled cell body. Viscerofugal neuron cell bodies were mapped using a pair of linear scales (AG-11; Mitutoyo Corporation, Japan) attached to the X and Y axes of the microscope stage. Figures were generated from grayscale images adjusted for contrast and brightness in Adobe Photoshop (CS5, Adobe Systems Inc, San Jose, CA) and were cropped and resized to improve display of cell bodies.

RESULTS

Distribution

Dense networks of extrinsic nerve fibres, as well as enteric viscerofugal neuron cell bodies were revealed by biotinamide applied to single colonic nerve trunks (7 preparations, n=5). Photomontages of biotinamide labelling are shown in **figure 5.01 and 5.02**. The immunohistochemistry of extrinsic nerve fibres was characterised in a separate series of experiments, described elsewhere (Chen et al., 2002). In the present study, 140 viscerofugal neurons (range 7-41 neurons; average 20 ± 11 neurons per preparation) were labelled with biotinamide; 3 neurons were excluded from morphological and immunohistochemical analysis as they were obscured by other viscerofugal neuron cell bodies.

Morphology

Axons of 57/137 viscerofugal neurons could be unequivocally distinguished from surrounding extrinsic nerve fibres, as they emerged from their cell bodies. All 57 viscerofugal neurons were uniaxonal; no instances of multipolar viscerofugal neurons were observed. In a minority of viscerofugal neurons, axonal varicose swellings occurred near the cell body (for example see **figure 5.04**, upper left micrograph; 14/57), while most had axons with a smooth appearance (43/57). Viscerofugal neuron cell bodies were smooth and round- or fusiform-shaped with a few or no dendrites (**figure 5.03 and 5.04**), or were irregular-shaped with multiple broad lamellar dendrites (**figure 5.05 and 5.06**). These morphologies resembled uniaxonal myenteric neurons described in small intestine as Dogiel type I “simple” and “lamellar” morphology, respectively (Furness et al., 1988). A cluster of

viscerofugal neurons, that include examples of both types of morphology is shown in **figure 5.06** (lower micrograph). Of 137 viscerofugal neurons, 77 had simple cell morphology and 60 were lamellar. Predictably, the cell bodies of simple cells were significantly smaller than lamellar cells, with a maximum area of vertical projection of $521 \pm 241\mu\text{m}^2$, compared to $767 \pm 235\mu\text{m}^2$ in Dogiel type I cell bodies ($p < 0.001$, independent samples t-test).

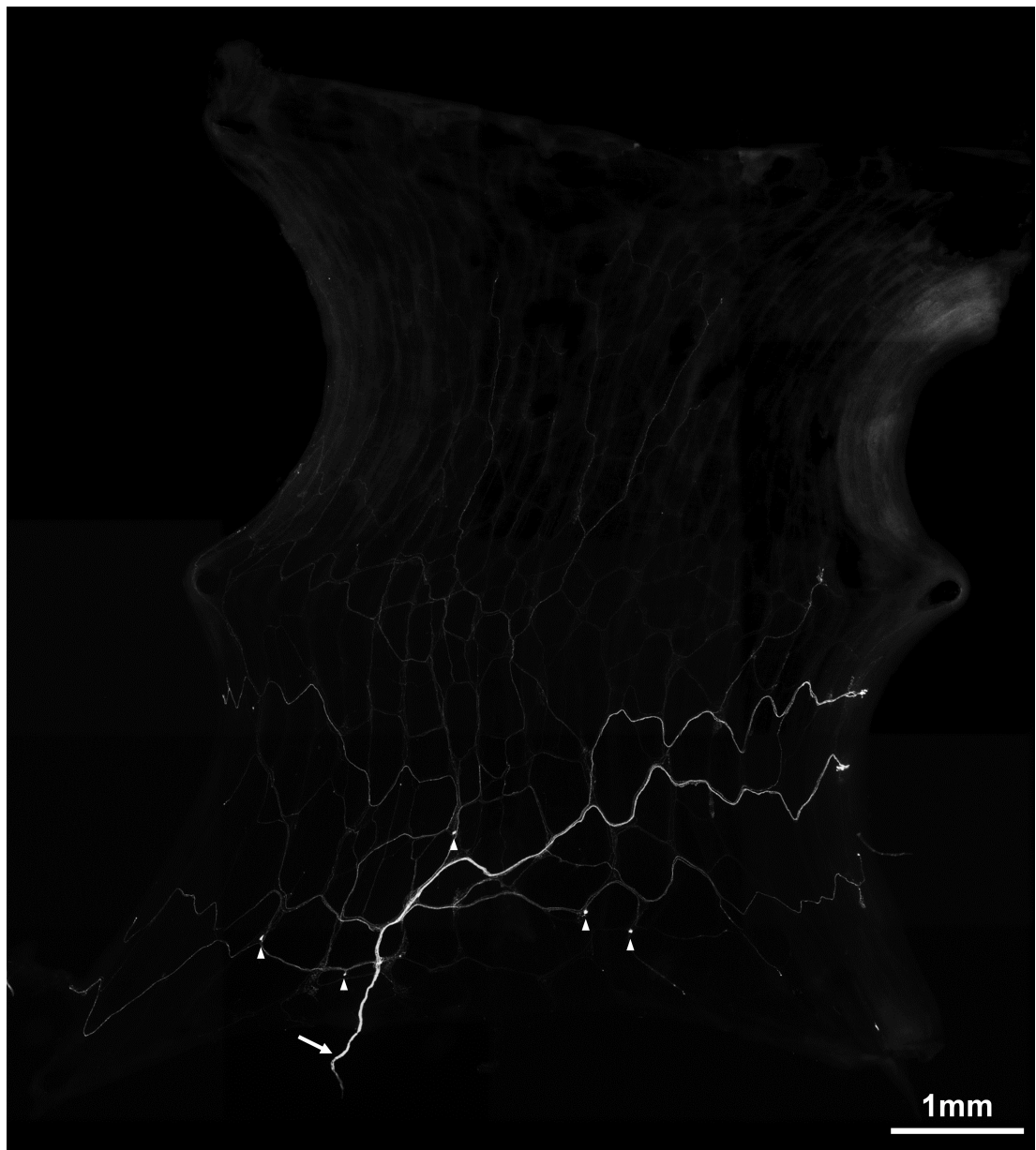


Figure 5.01

Example of biotinamide labelling from a colonic nerve trunk in a wholemount preparation of guinea pig distal colon. Numerous fine extrinsic nerve fibres arising from the labelled colonic nerve trunk (see arrow) can be seen coursing throughout the myenteric plexus. Several viscerofugal nerve cell bodies were labelled and may be seen in this low power micrograph (these are marked with arrowheads).

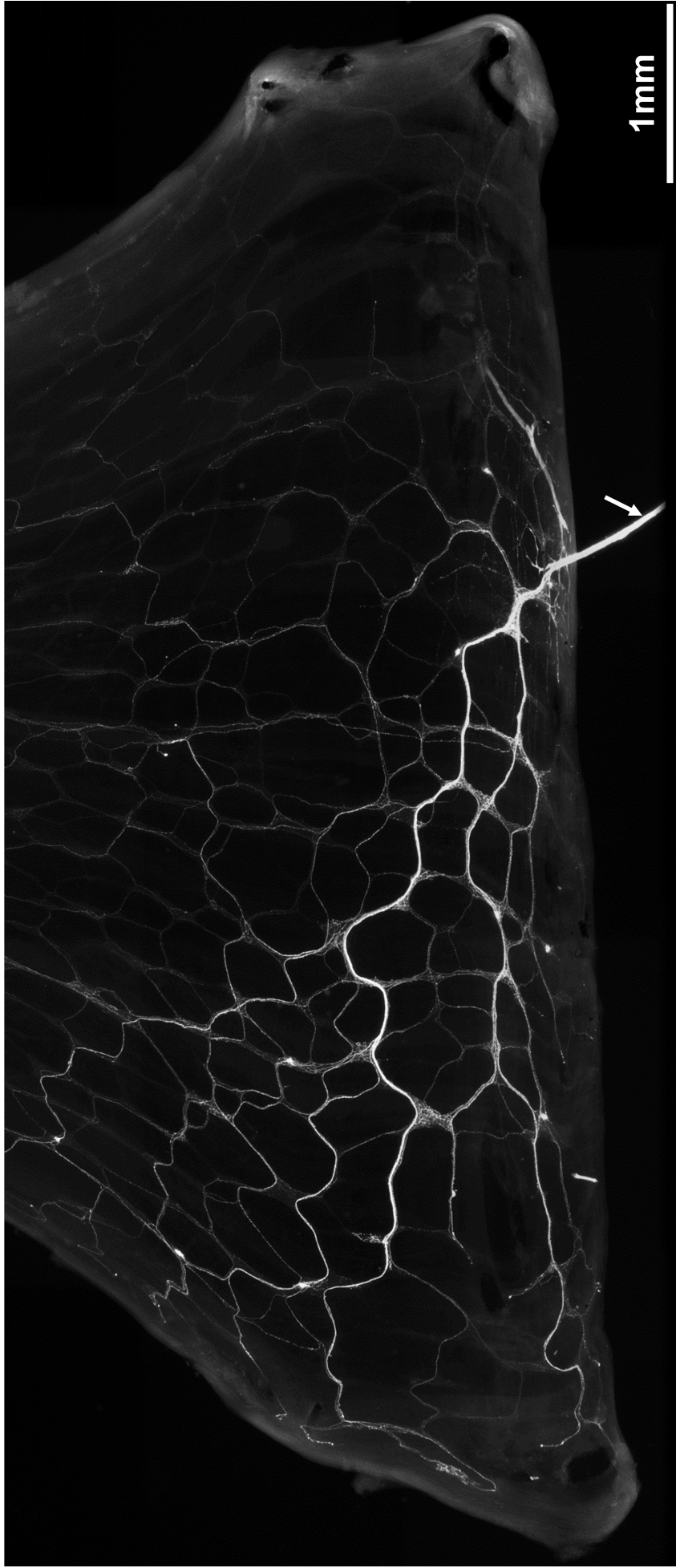


Figure 5.02

Expanded view of biotinamide labelling from a single colonic nerve trunk. Dense labelling of numerous fine varicose fibres can be seen ramifying within myenteric ganglia. Multiple intensely labelled viscerofugal neurons can also be seen. The arrow indicates the colonic nerve trunk from which the viscerofugal neurons and extrinsic nerve fibres were labelled.

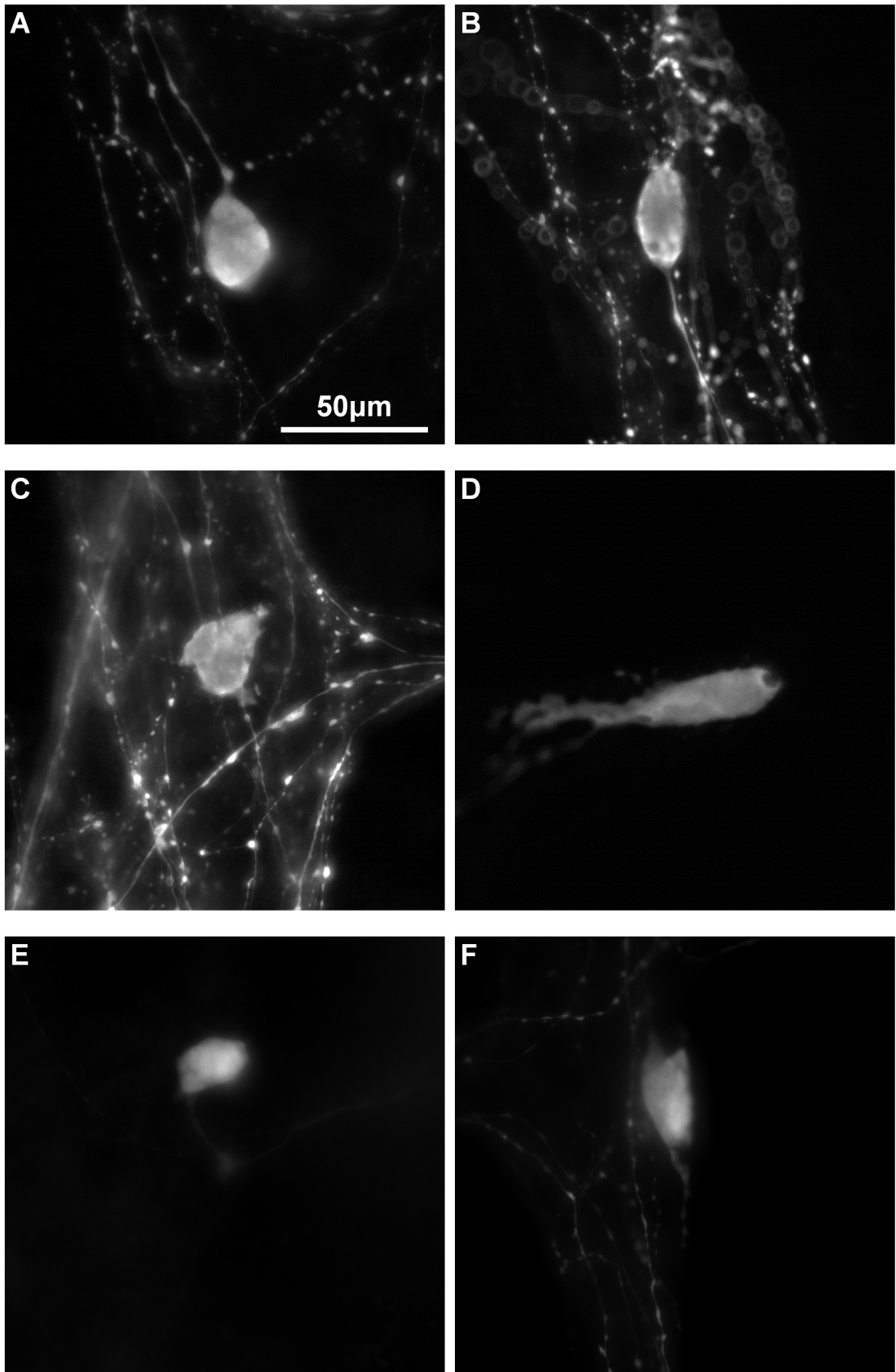


Figure 5.03

Fluorescence micrographs of viscerofugal neuron cell bodies with Dogiel type I “simple” cell morphology, labelled A-F. These cells were small and ovoid- or fusiform-shaped and had a few or no dendrites.

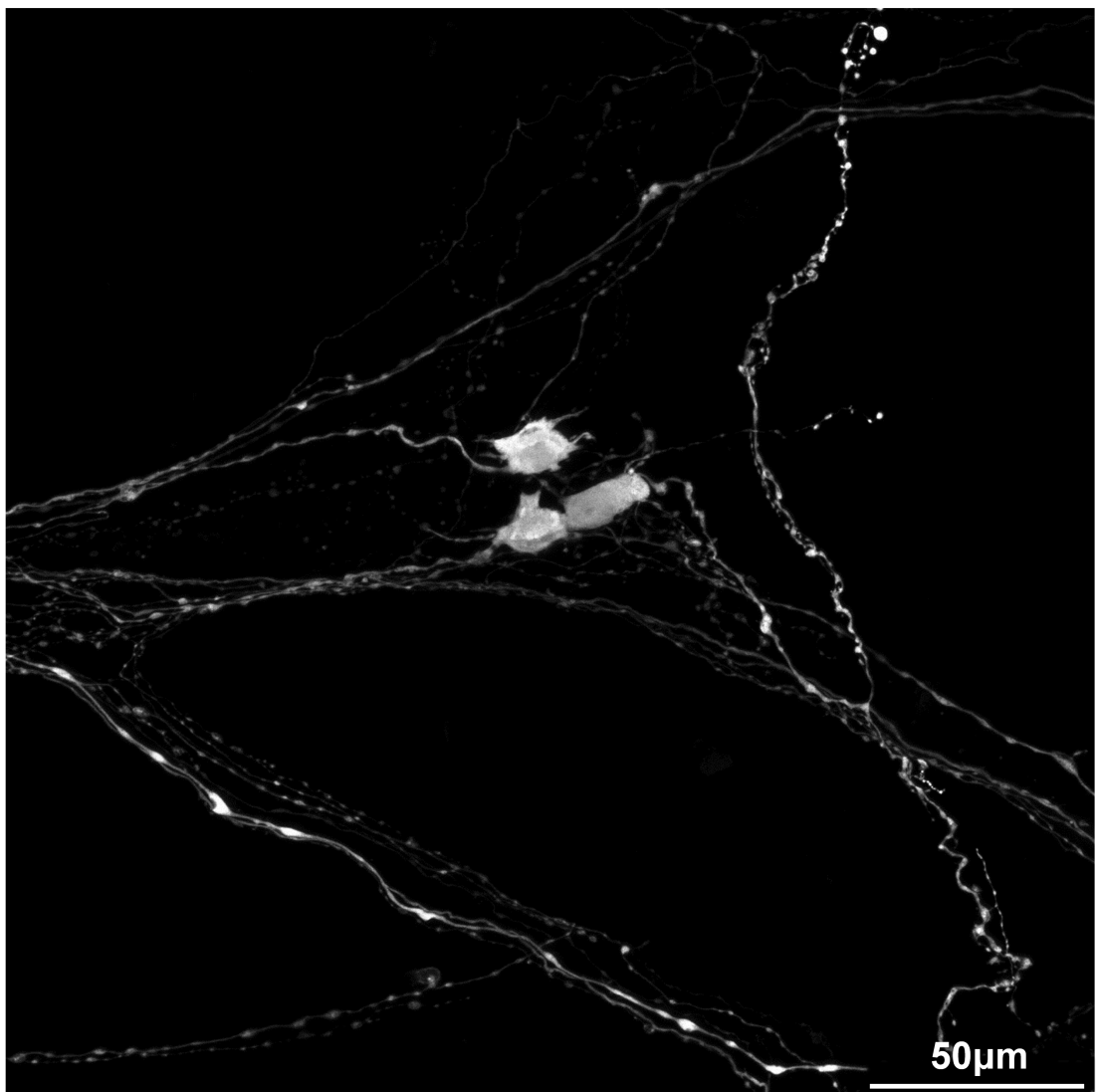
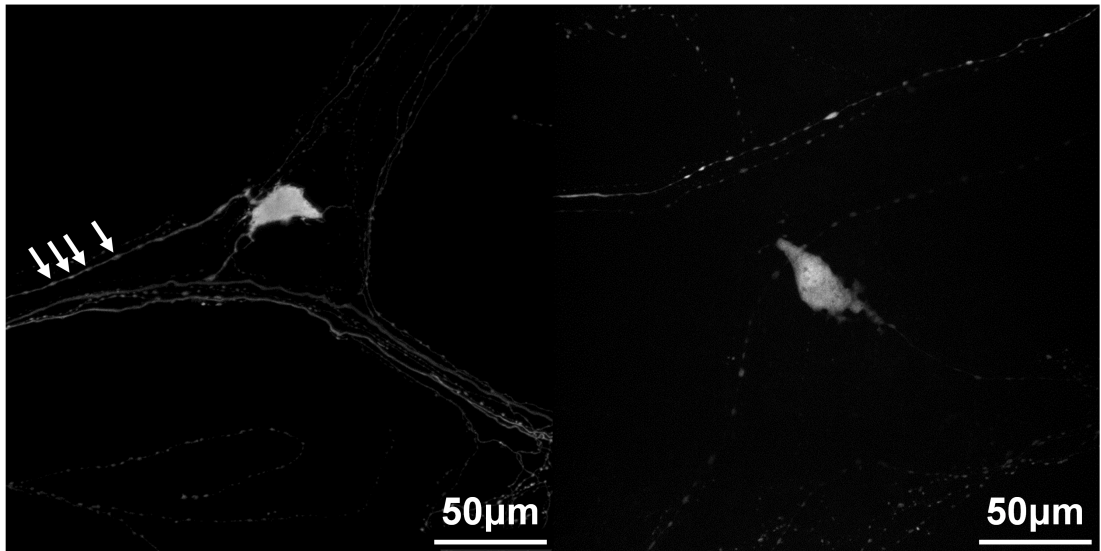


Figure 5.04

Confocal maximum intensity Z-stacks of viscerofugal neurons with Dogiel type I “simple” cell morphology. Note that swellings can be seen on the axon of the viscerofugal neuron in the upper left micrograph (arrows).

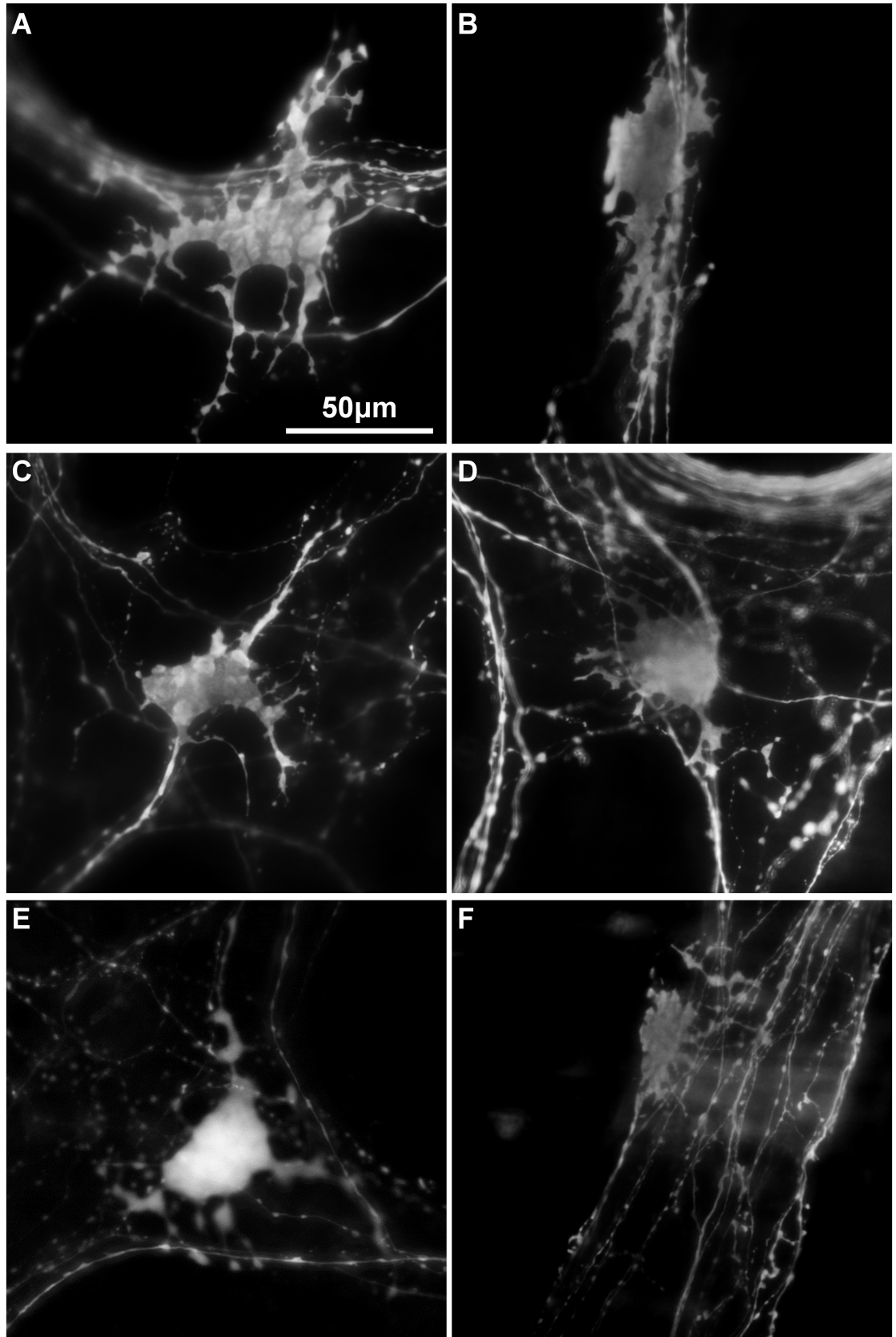


Figure 5.05

Fluorescence micrographs of biotinamide-labelled viscerofugal neuron cell bodies with Dogiel type I “lamellar” soma-dendritic morphology (A-F). These cells typically had several flat “lamellar” dendrites, and irregularly-shaped cell bodies.

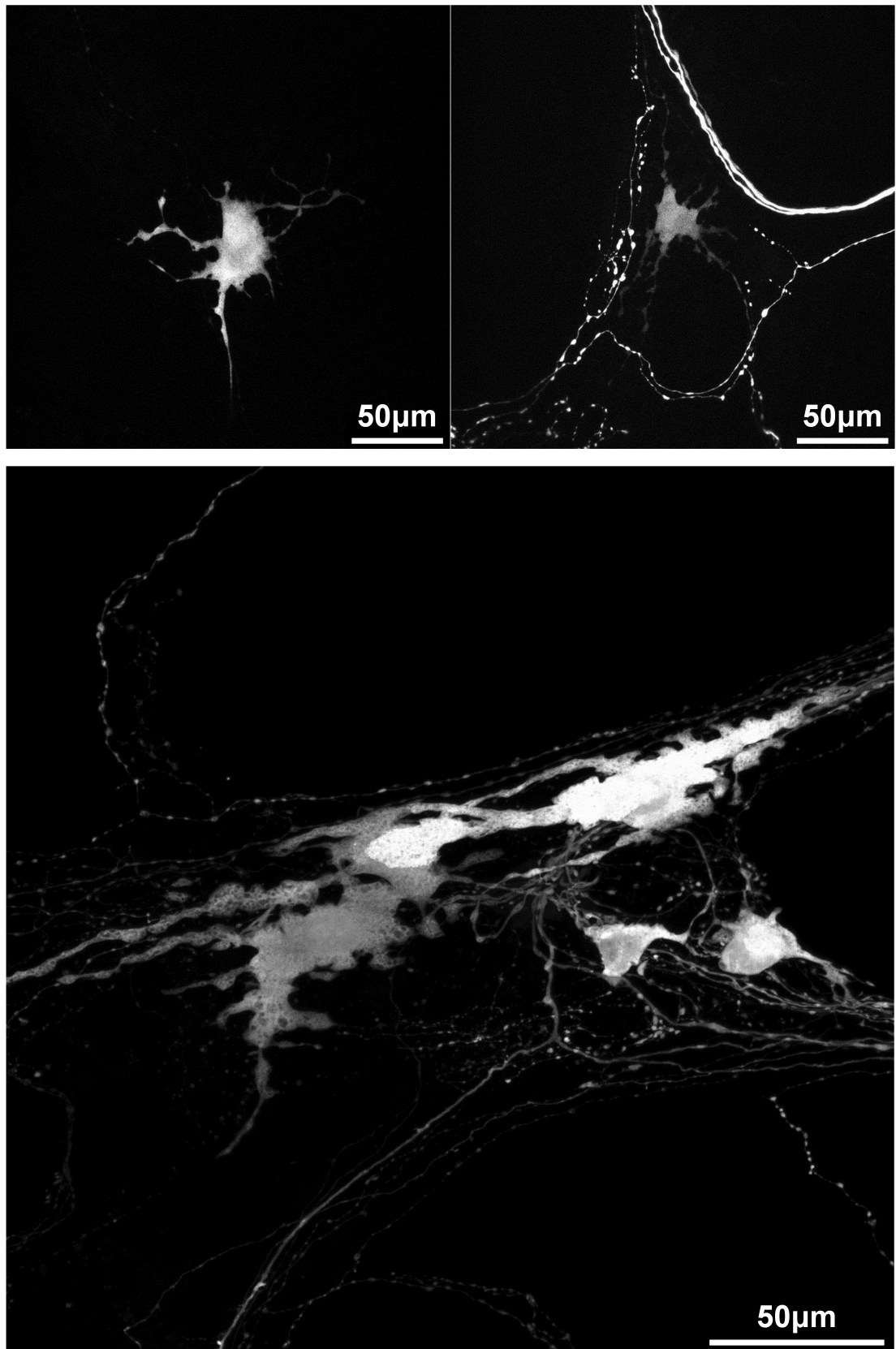


Figure 5.06

Confocal maximum intensity Z-stacks of viscerofugal neurons with Dogiel type I “lamellar” cell morphology. The lower micrograph also shows two nearby viscerofugal neurons with simple cell morphology for comparison.

ChAT and NOS immunoreactivity

Preparations were labelled with antisera against the neurotransmitter synthesizing enzymes choline acetyltransferase (ChAT) and nitric oxide synthase (NOS). As has been previously reported (Mann et al., 1995), viscerofugal neurons either contained ChAT-immunoreactivity alone in their cell bodies (**figure 5.07**), or contained both ChAT- and NOS-immunoreactivity (**figure 5.08**). However, there were also a few biotinamide-labelled cell bodies that contained NOS-immunoreactivity alone (**figure 5.09**), or did not contain either NOS- or ChAT-immunoreactivity (**figure 5.10**). Of 137 biotinamide-labelled viscerofugal cell bodies ($n = 5$), 127 (82%) were immunoreactive for either ChAT or NOS. ChAT+/NOS- cell bodies made up 60 of 137 (44%), 15 of 137 (11%) were NOS+/ChAT-, 52 of 137 (38%) were ChAT+/NOS+, and 10 of 137 were NOS-/ChAT- (7%). These data are displayed in **figure 5.11A** and **5.11B**.

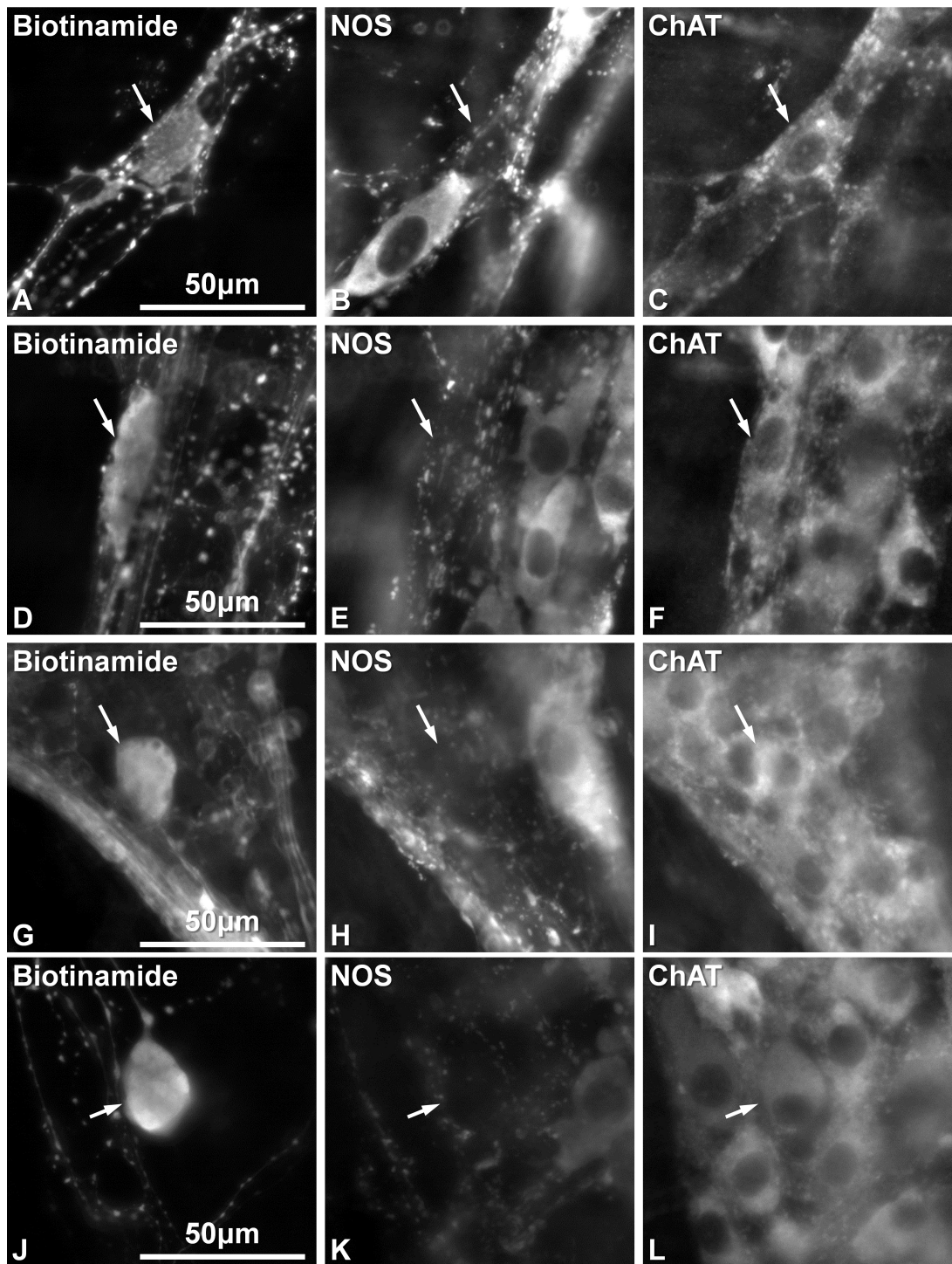


Figure 5.07

Matched micrographs of biotinamide labelled viscerofugal neurons, NOS immunoreactivity, and ChAT immunoreactivity. These micrographs show examples of ChAT+/NOS- viscerofugal nerve cell bodies. ChAT, but not NOS fluorescence is visible within each cell body.

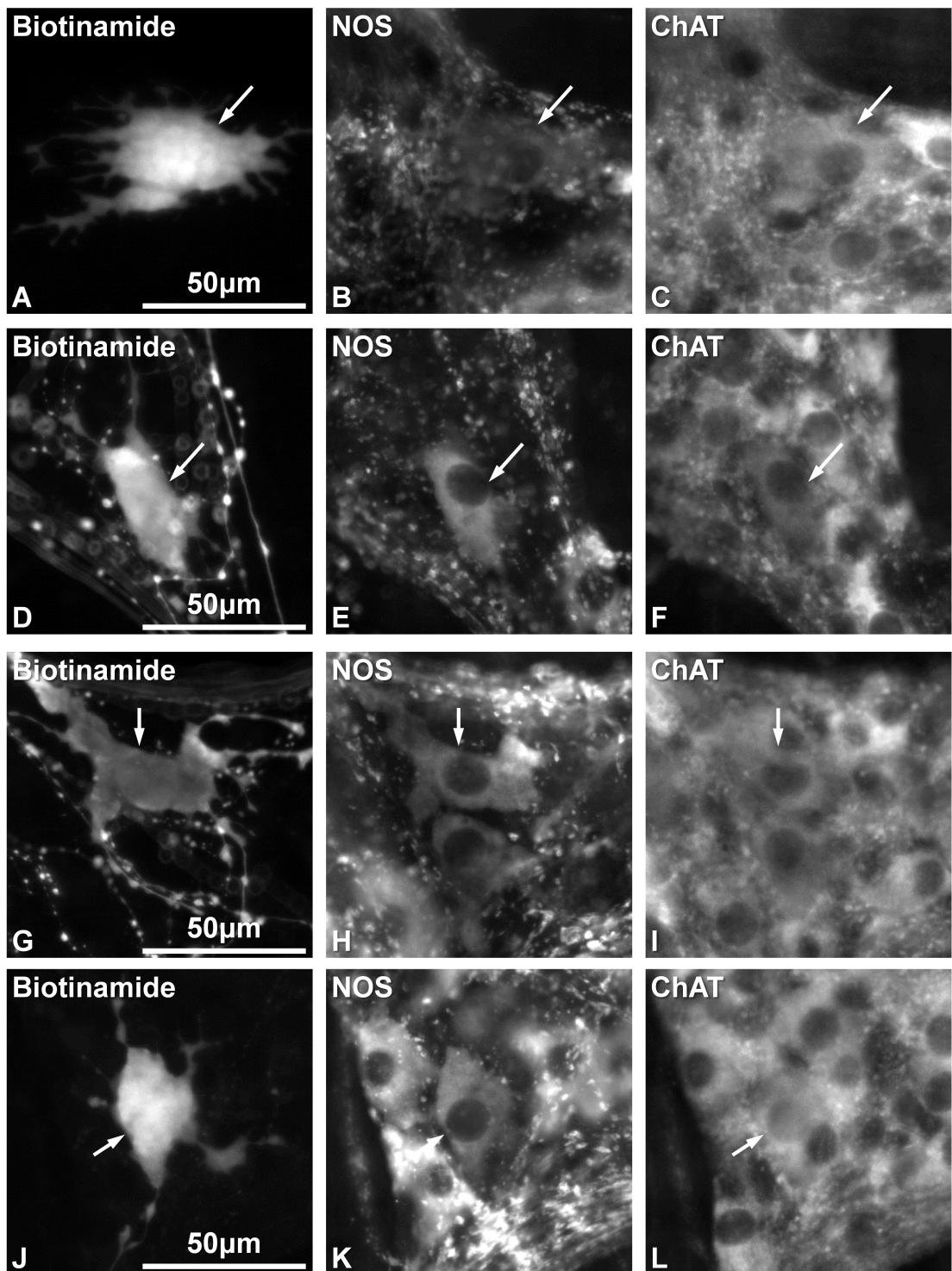


Figure 5.08

Matched micrographs of biotinamide labelled viscerofugal neurons, NOS immunoreactivity, and ChAT immunoreactivity. These micrographs show examples of ChAT+/NOS+ viscerofugal nerve cell bodies. Both ChAT and NOS fluorescence is visible within each cell body.

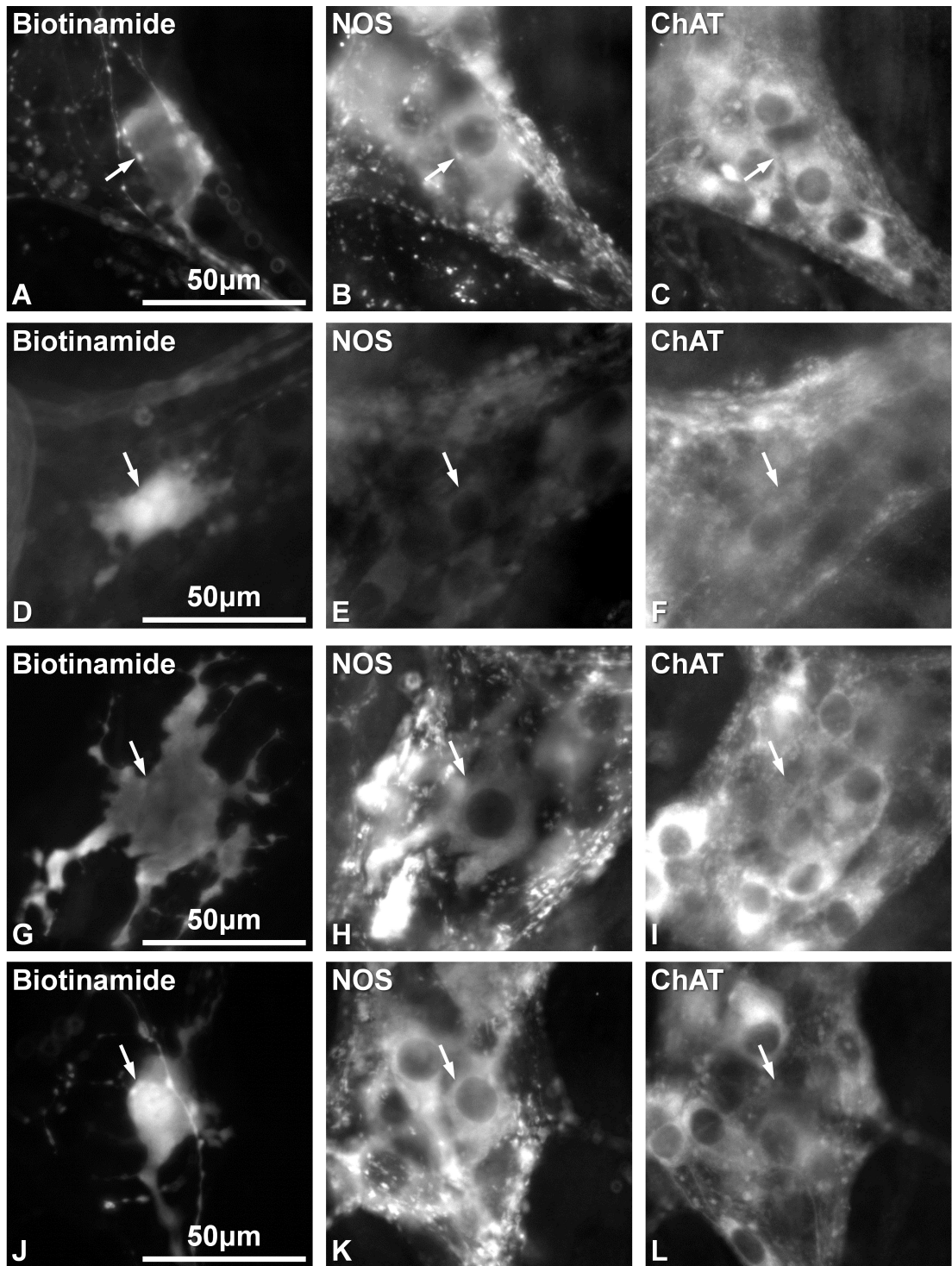


Figure 5.09

Matched micrographs of biotinamide labelled viscerofugal neurons, NOS immunoreactivity, and ChAT immunoreactivity. These micrographs show examples of ChAT-/NOS+ viscerofugal nerve cell bodies. Immunoreactivity for NOS, but not ChAT is visible within each cell body.

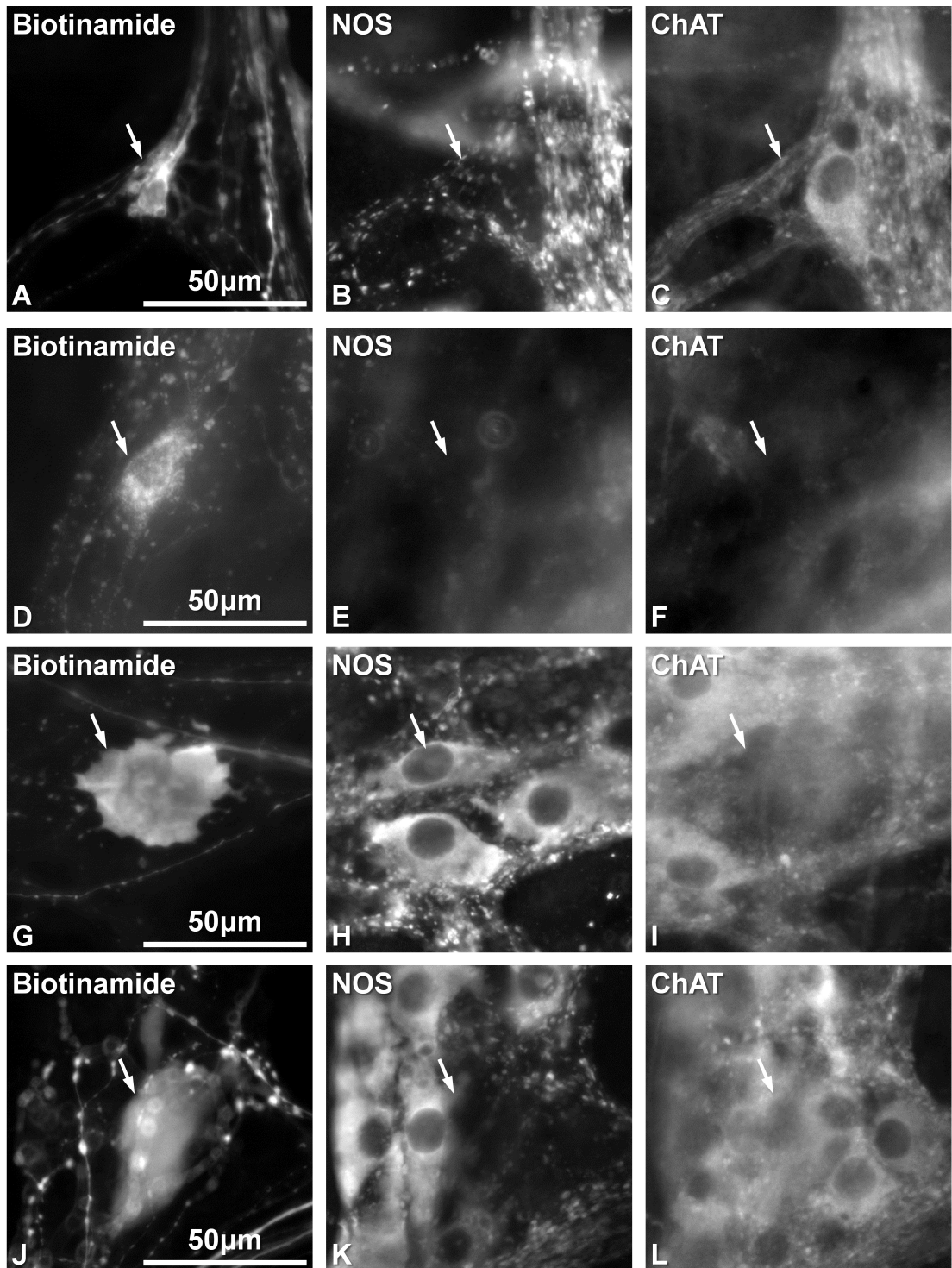


Figure 5.10

Matched micrographs of biotinamide labelled viscerofugal neurons, NOS immunoreactivity, and ChAT immunoreactivity. These micrographs show examples of ChAT-/NOS- viscerofugal nerve cell bodies. Both ChAT and NOS fluorescence are lacking within each cell body.

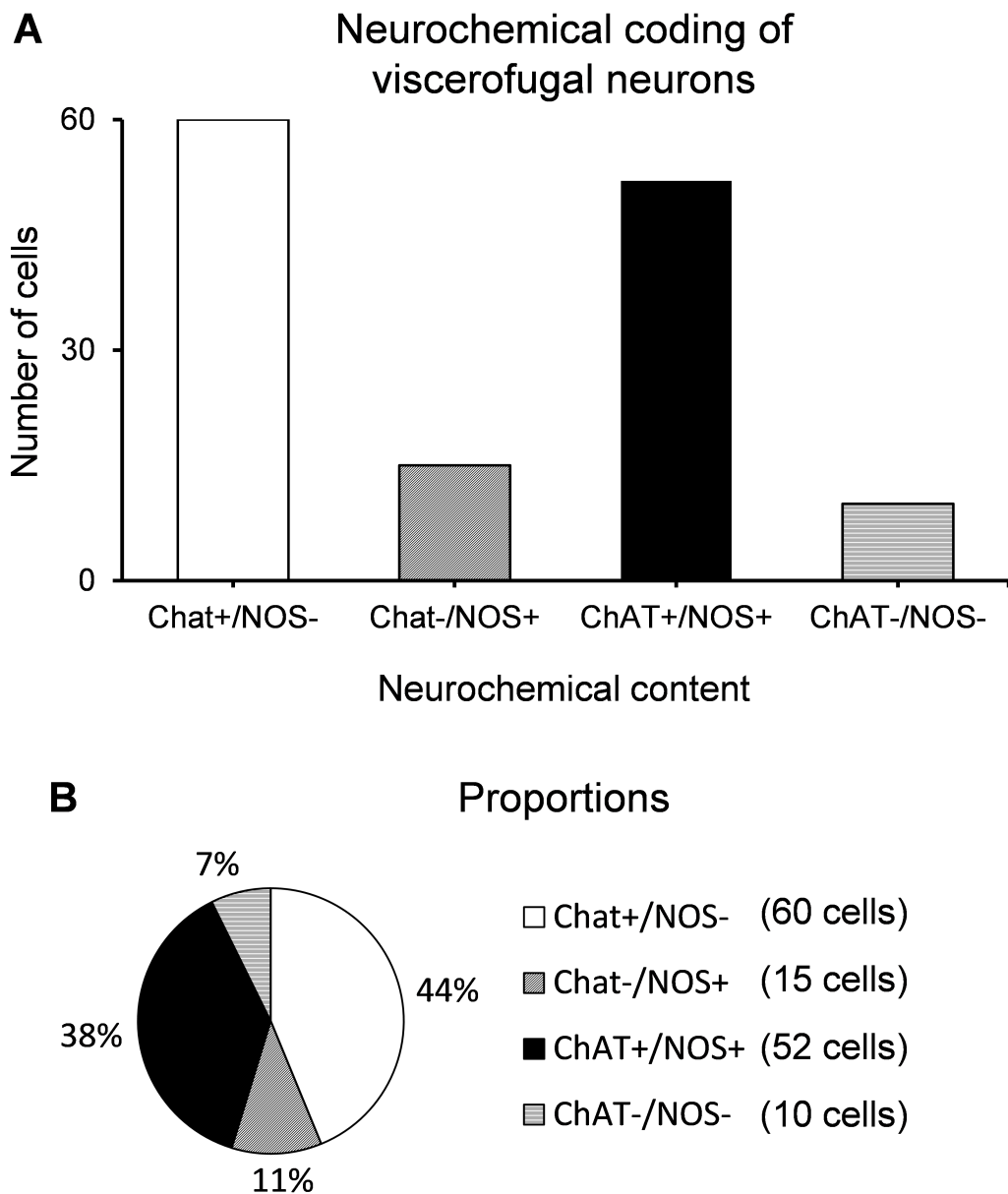


Figure 5.11

The numbers and proportion of viscerofugal neurons containing different combinations of ChAT and NOS immunoreactivity. (A) Numbers (B) Proportions. The most prominent groups were ChAT+/NOS- neurons and ChAT+/NOS+ neurons, which have been identified previously. Two previously unreported groups of viscerofugal neurons lacked ChAT and NOS, or contained NOS alone. These groups comprised 18% of all viscerofugal neurons.

Chemical coding and nerve cell body morphology

Dogiel type I simple and lamellar morphologies did not occur equally among the different neurochemically coded groups of viscerofugal neurons. An abundance of ChAT+/NOS- neurons had simple cell morphology, while most of the ChAT+/NOS+ neurons had lamellar morphologies (**figure 5.12A**). There were statistically significant associations between chemical code and cell body morphology ($X^2=38.4$, df: 4, $p<0.05$): ChAT+/NOS- coding was associated with simple soma-dendritic morphology (standardized residual: 2.4); ChAT+/NOS+ coding was associated with lamellar soma-dendritic morphology (standardized residual: 3.5). ChAT-/NOS+ and ChAT-/NOS- viscerofugal neurons were not significantly associated with either type of morphology (both had standardized residuals $< |2|$, and thus did not significantly deviate from expected values).

Consistent with the aforementioned differences in cell body sizes between simple and lamellar morphologies, ChAT+/NOS- neurons, which were mostly simple cells, were significantly smaller than ChAT+/NOS+ neurons, which were mostly lamellar ($446 \pm 203 \mu\text{m}^2$ vs $803 \pm 189 \mu\text{m}^2$, respectively, one-way ANOVA, Bonferroni post-test, $p<0.001$, **figure 5.12B** and **5.13A**). A frequency histogram of cell body sizes, comparing the ChAT+/NOS- and ChAT+/NOS+ populations is shown in **figure 5.13B**. The two less numerous groups of viscerofugal neurons (ChAT-/NOS+ and ChAT-/NOS-) were not significantly different in cell body size.

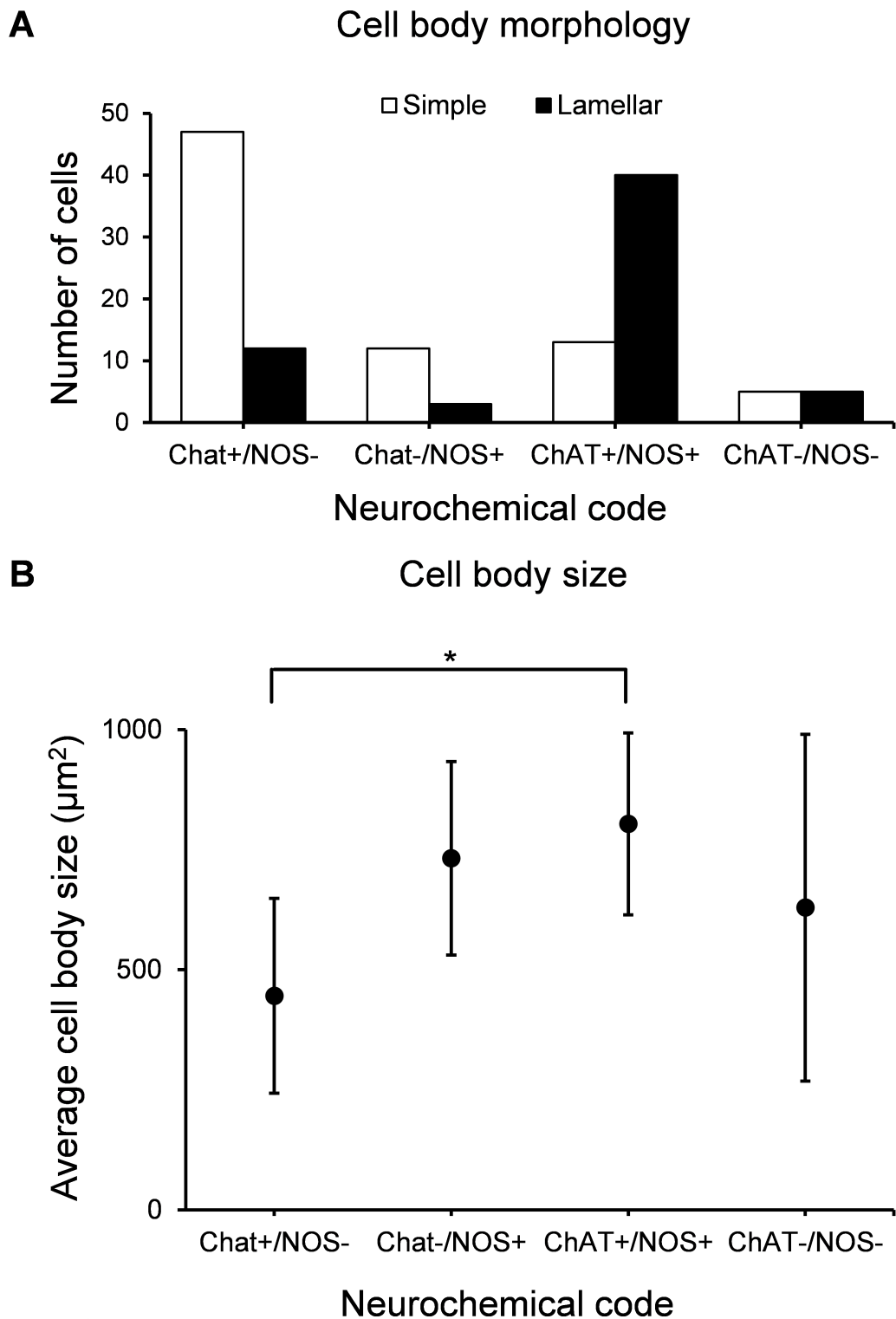


Figure 5.12

(A) Morphology and size of viscerofugal neurons with different combinations of immunoreactivity to ChAT and NOS. Simple morphology was significantly associated with ChAT+/NOS- chemical coding; lamellar morphology was associated with ChAT+/NOS+ chemical coding. Morphology was not associated with either of the smaller chemically coded groups. (B) Average cell body size of each chemically coded group of viscerofugal neurons. ChAT+/NOS+ viscerofugal neurons were significantly larger than ChAT+/NOS- neurons (* $p < 0.001$, one-way ANOVA, Bonferroni post-test).

Viscerofugal nerve cell body size and neurochemical code

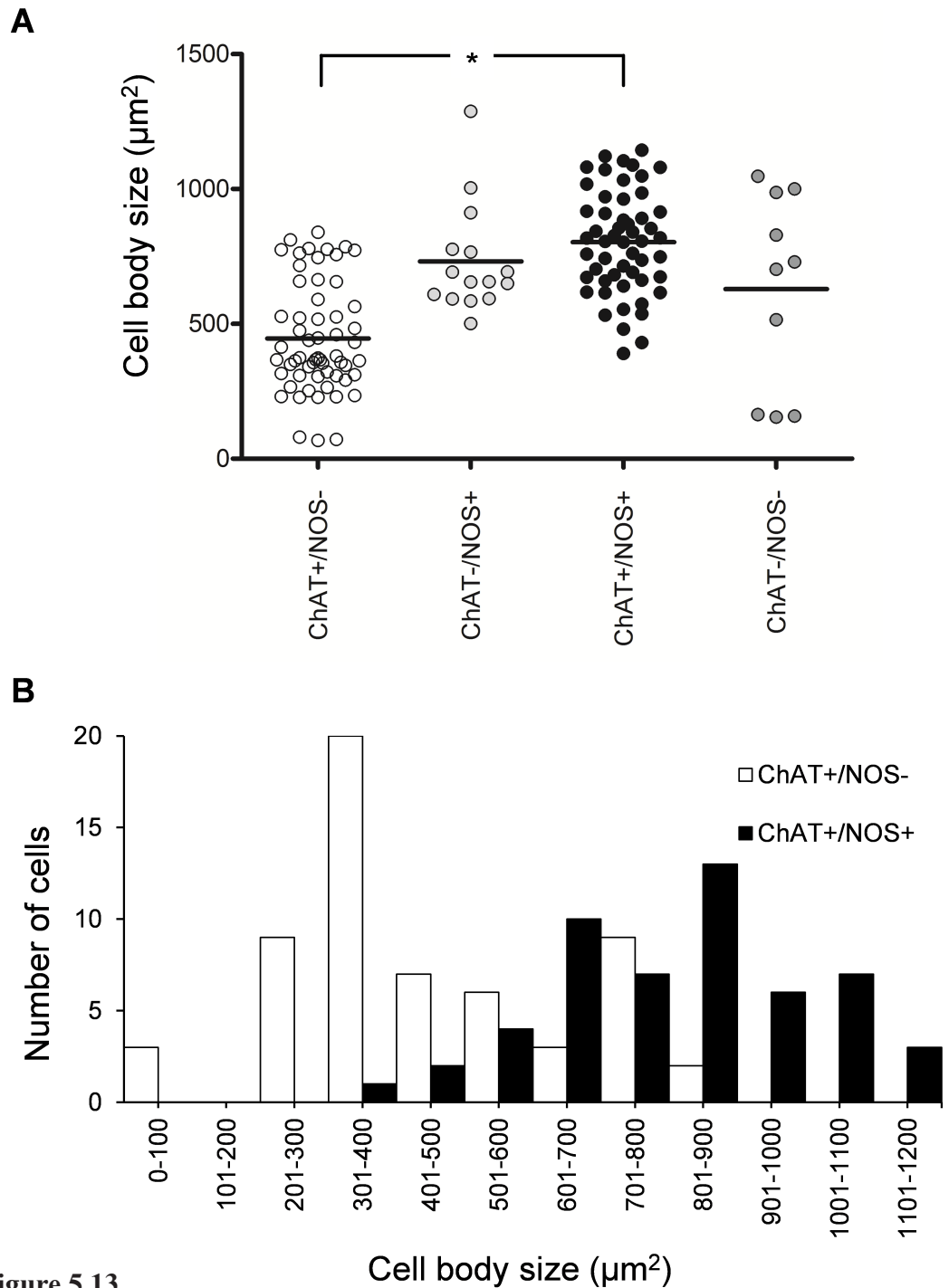


Figure 5.13

(A) The cell body size of each chemically coded group of viscerofugal neurons, showing all individual cases. ChAT+/NOS+ neurons were significantly larger than ChAT+/NOS- neurons (* $p < 0.001$, one-way ANOVA, Bonferroni post-test). The horizontal bars indicate the mean. (B) Clustered frequency histogram of cell body sizes for the two most numerous groups of viscerofugal neurons: ChAT+/NOS+ neurons and ChAT+/NOS- neurons. Both populations form normal distributions around different peaks.

Chemical code and spatial distribution

Most viscerofugal neuron cell bodies were located within a few millimetres of the mesenteric border. This preferential distribution of viscerofugal neuron cell bodies toward the mesenteric border has been repeatedly observed in the colon across multiple species (Furness et al., 1990c, Barbiers et al., 1993, Luckensmeyer and Keast, 1995a, Miller and Szurszewski, 2002). However, visual examination of biotinamide-labelled preparations suggested that many of the viscerofugal neurons located further away from the mesenteric border were also greater in cell body size and had lamellar soma-dendritic morphology. We therefore mapped the spatial distribution of viscerofugal neuron cell bodies, and compared it with their neurochemical content (**figure 5.14**). Consistently, ChAT+/NOS+ viscerofugal neurons were distributed more widely in the circumferential axis across the gut wall than ChAT+/NOS- neurons, which tended to be concentrated at the mesenteric border (e.g. 30%, compared to 70% were located within 2mm of the mesenteric border, respectively; see **figure 5.14**). Thus, ChAT+/NOS+ neurons were on average located further from the mesenteric border than ChAT+/NOS- neurons ($3.5 \pm 2.2\text{mm}$ vs $1.9 \pm 1.8\text{mm}$, respectively, $p < 0.001$, Bonferroni post-test, one-way ANOVA). In addition, the total distance of viscerofugal neuron cell bodies from colonic nerve entry was greater for ChAT+/NOS+ neurons than ChAT+/NOS- neurons ($5.0 \pm 2.3\text{mm}$ vs $3.1 \pm 2.0\text{mm}$, respectively, $p < 0.001$, Bonferroni post-test, one-way ANOVA, **figure 5.15A**). **Figure 5.15B** shows a graph of cell body size plotted against its distance from the colonic nerve within the gut. Larger cell bodies tended to be further away.

The longitudinal distributions of ChAT+/NOS+ and ChAT+/NOS- viscerofugal neurons was different, relative to the point of entry of the labelled nerve trunk. ChAT+/NOS+ neurons tended to descend to the colonic nerve trunk from which they were labelled (i.e. they had aborally projecting axons). ChAT+/NOS- neurons on the other hand, had axons that tended to ascend (orally projecting) to the labelled nerve trunk (**figure 5.14**). On average, ChAT+/NOS+ viscerofugal nerve cell bodies were 1.5 ± 3.5 mm to the oral side of nerve trunks and ChAT+/NOS- viscerofugal nerve cell bodies were 1.3 ± 2.2 mm to the aboral side ($p < 0.001$, Bonferroni post-test, one-way ANOVA).

The spatial distribution of viscerofugal nerve cell bodies labelled from colonic nerves in the distal colon

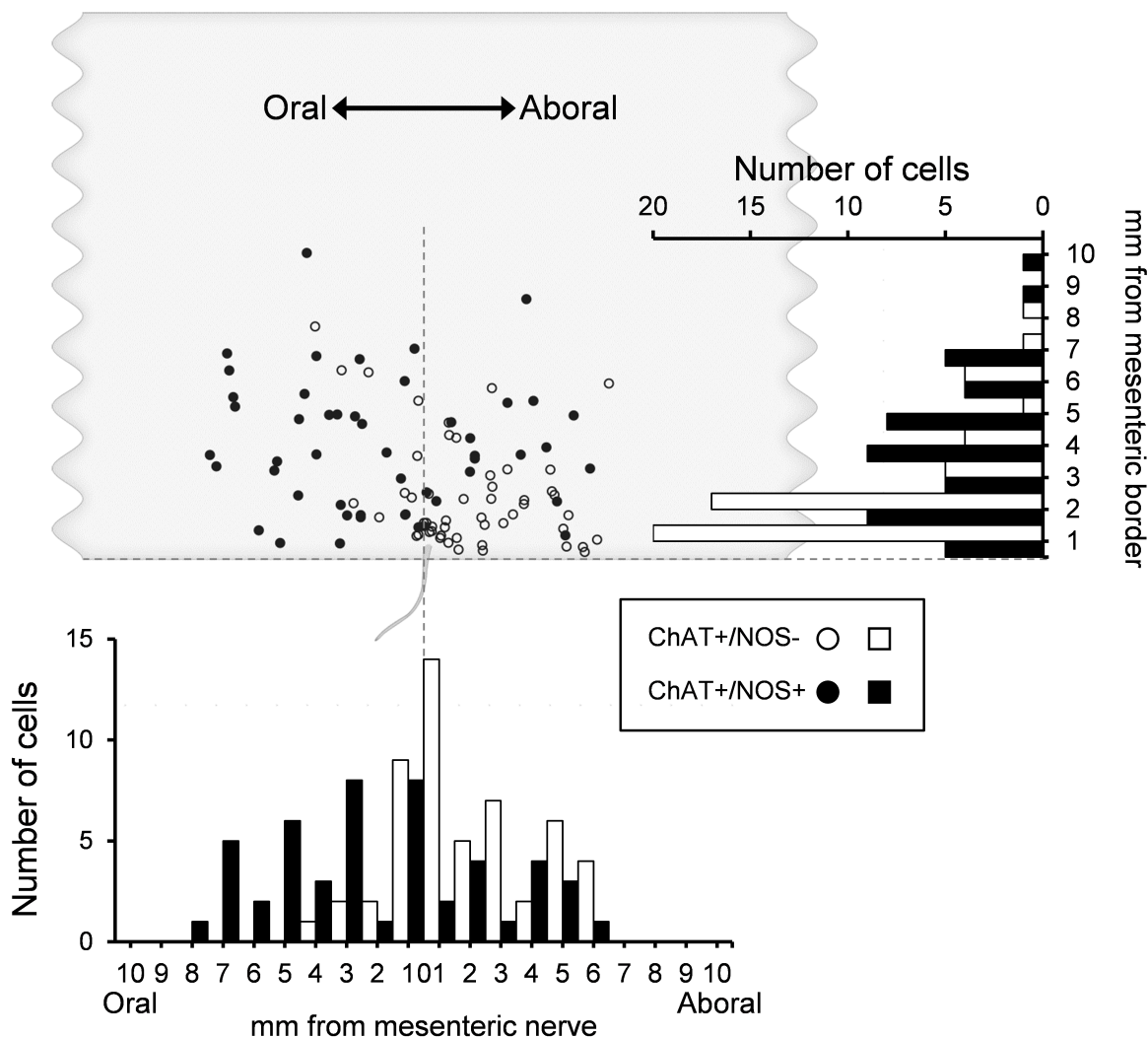
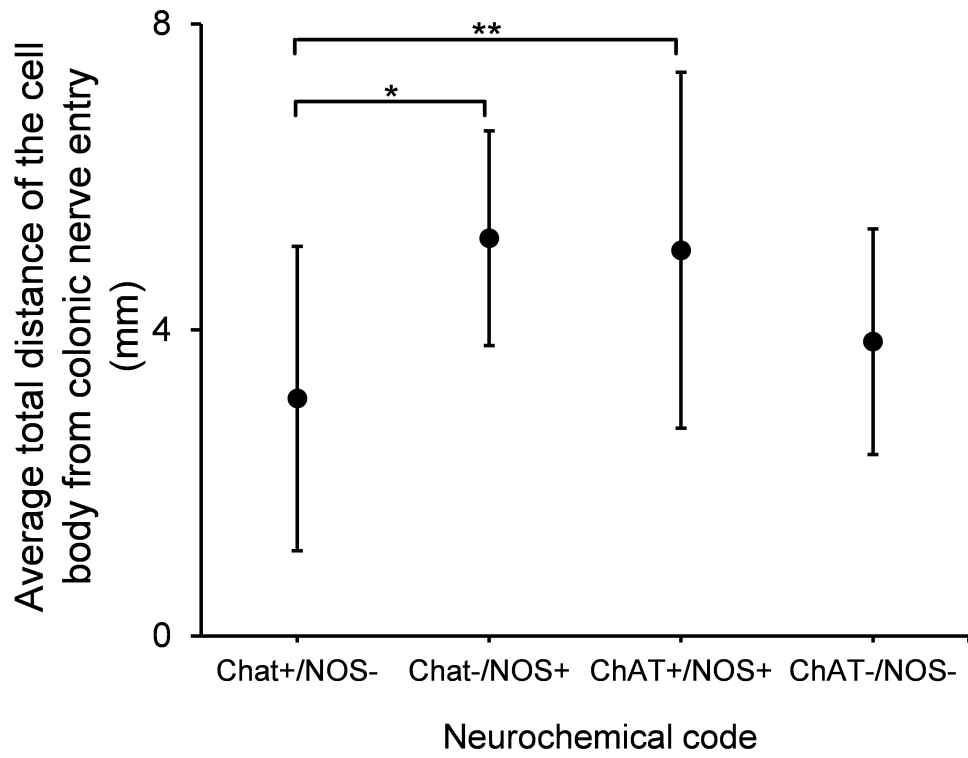


Figure 5.14

The spatial distribution of viscerofugal nerve cell bodies in guinea pig distal colon. This figure shows a composite map of the locations of viscerofugal nerve cell bodies labelled in 7 preparations (n=5). Frequency histograms (adjacent) show the circumferential and longitudinal distribution of the different chemically coded groups of viscerofugal neurons. Full black circles and bars indicate ChAT+/NOS+ neurons; open circles and bars indicate ChAT+/NOS- neurons. The cell bodies of ChAT+/NOS+ viscerofugal neurons are distributed relatively evenly in the circumferential axis compared to ChAT+/NOS- neurons, which tend to be clustered close to the colonic nerve (mesenteric border). In addition, ChAT+/NOS+ neurons show a peak in their distribution oral to the colonic nerve, compared with ChAT+/NOS- neurons which peak aborally. The dashed lines indicate the point of nerve entry in both axes.

A



B

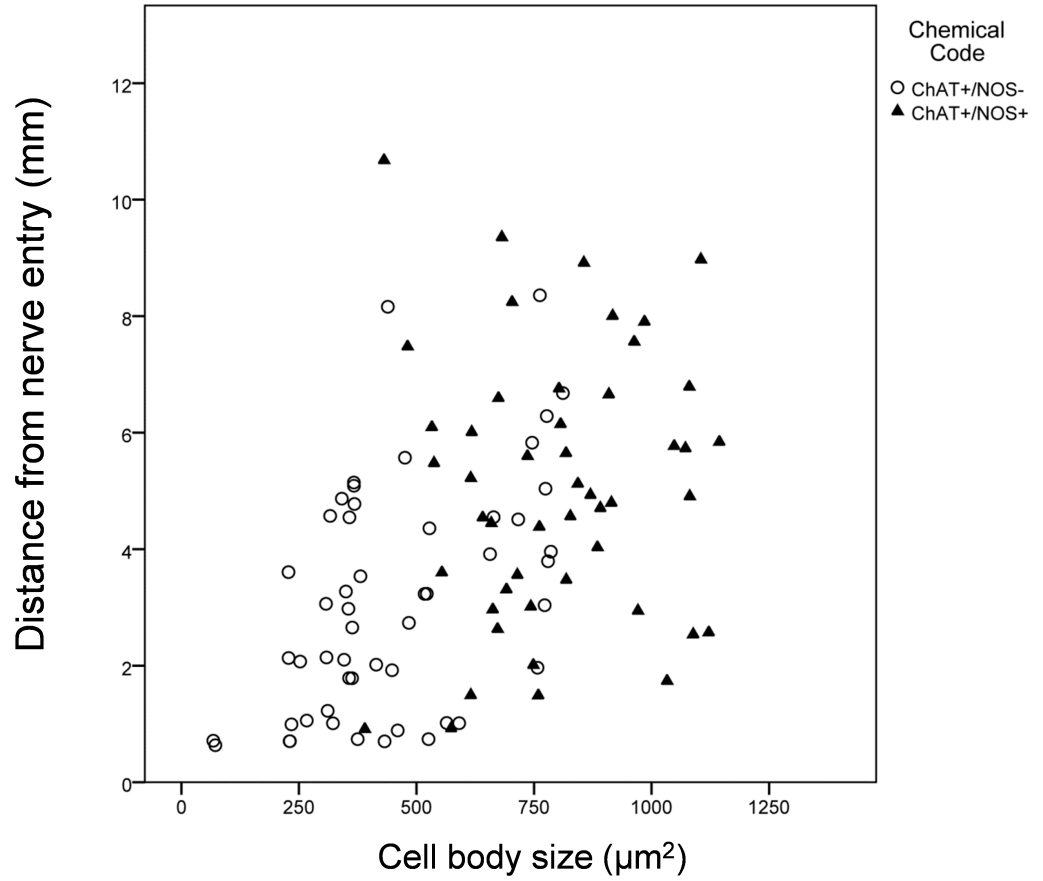


Figure 5.15 see next page for figure legend

Figure 5.15

(A) The average total distance of cell bodies to colonic nerves for each chemically coded group of viscerofugal neurons. Similar to the circumferential distribution, ChAT+/NOS+ neurons were significantly further in the gut, from the colonic nerve through which their axons projected than ChAT+/NOS- neurons (** $p < 0.001$, bonferroni post-test, one-way ANOVA). In addition, the other group of viscerofugal neurons that contained NOS also had cell bodies that were on average further from colonic nerve trunks, compared to ChAT+/NOS- neurons (* $p < 0.05$ bonferroni post-test, one-way ANOVA). (B) Viscerofugal neuron cell body size plotted against their distance from the colonic nerve entry to the gut. Large cell bodies tended to be further from their colonic nerves, and vice versa.

Viscerofugal neurons in the small intestine

Retrograde neuronal tracing from prevertebral ganglia combined with immunohistochemistry showed that most viscerofugal neurons in the small intestine contain ChAT, but lack NOS immunoreactivity. Thus, we were interested in whether viscerofugal neurons in the small intestine were morphologically similar to the population of ChAT+/NOS- viscerofugal neurons in the colon. Sixty-six viscerofugal neurons were labelled from mesenteric nerves to preparations of guinea pig ileum using biotinamide (15 preparations, n=13). Fewer viscerofugal neurons were labelled per preparation in ileum than in colon (range 2-13 neurons; average 4 ± 3 neurons per preparation, compared to 20 ± 11 in the colon). The viscerofugal neurons that were labelled had small ovoid- or fusiform-shaped cell bodies, and were clustered tightly near the mesenteric border. In total, 58/66 viscerofugal neurons had simple cell body morphology; 8 were classified as lamellar (examples are shown in **figure 5.16**; numbers are shown in **figure 5.17A**). The proportion of viscerofugal neurons in the ileum with simple and lamellar cell body morphology are shown in **figure 5.17B**. The size of cell bodies of viscerofugal neurons in the ileum were similar to ChAT+/NOS- colonic viscerofugal neurons, with a maximal vertical projection area of $422 \pm 191 \mu\text{m}^2$ and they were significantly smaller than ChAT+/NOS+ colonic viscerofugal neurons ($p < 0.001$, Bonferroni post -test, one-way ANOVA). This is reflected in the distribution of cell body sizes among these 3 groups of viscerofugal neurons, shown in **figure 5.18**. Around the circumference of the gut, viscerofugal neurons in ileum were tightly clustered at the mesenteric border (94% within 2mm; **figure 5.19**). Longitudinally, viscerofugal neurons were distributed evenly about the nerve entry point, showing neither an oral or aboral bias (average position: $0.1 \pm 2.1\text{mm}$ aboral, **figure 5.19**).

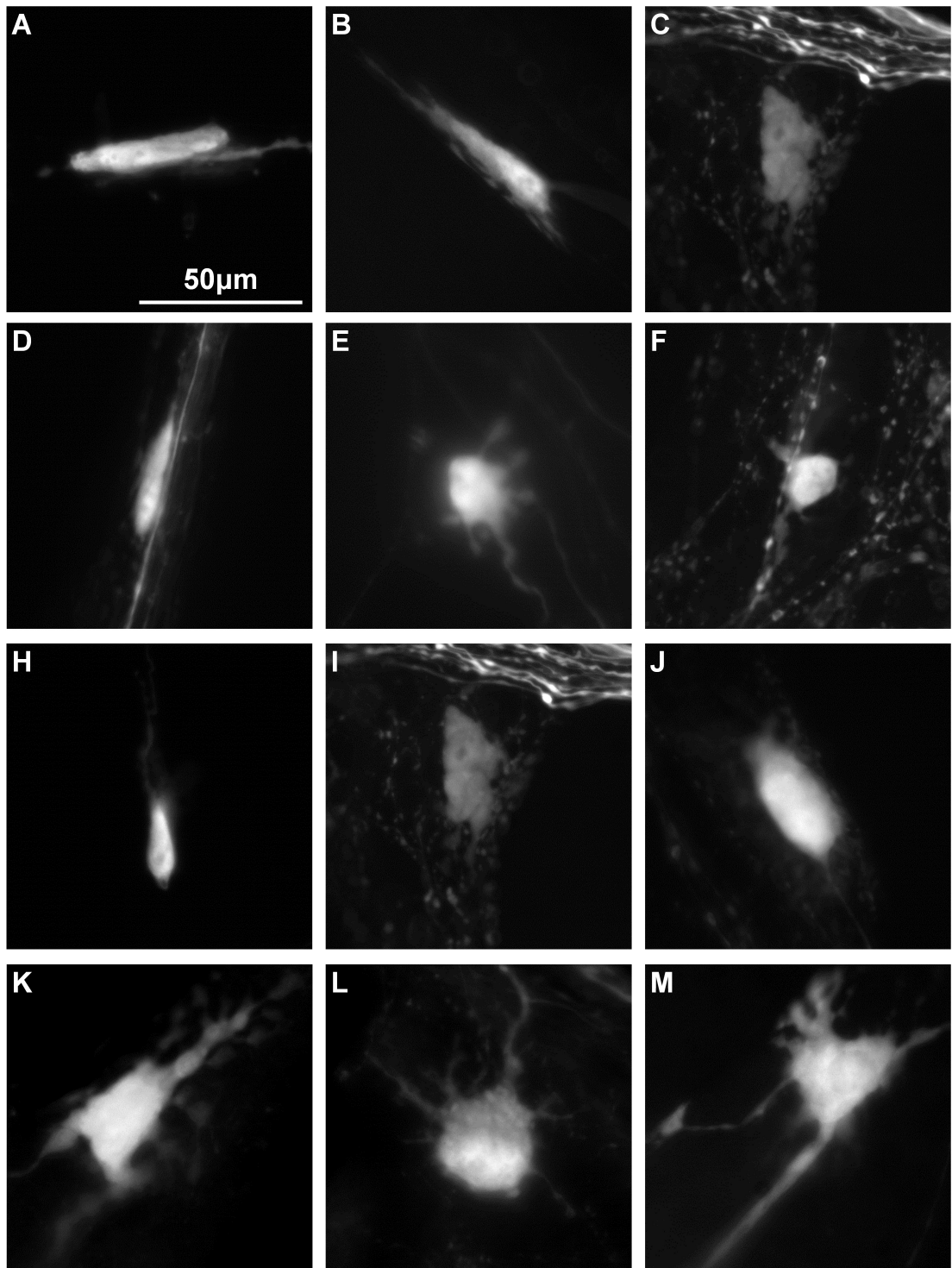
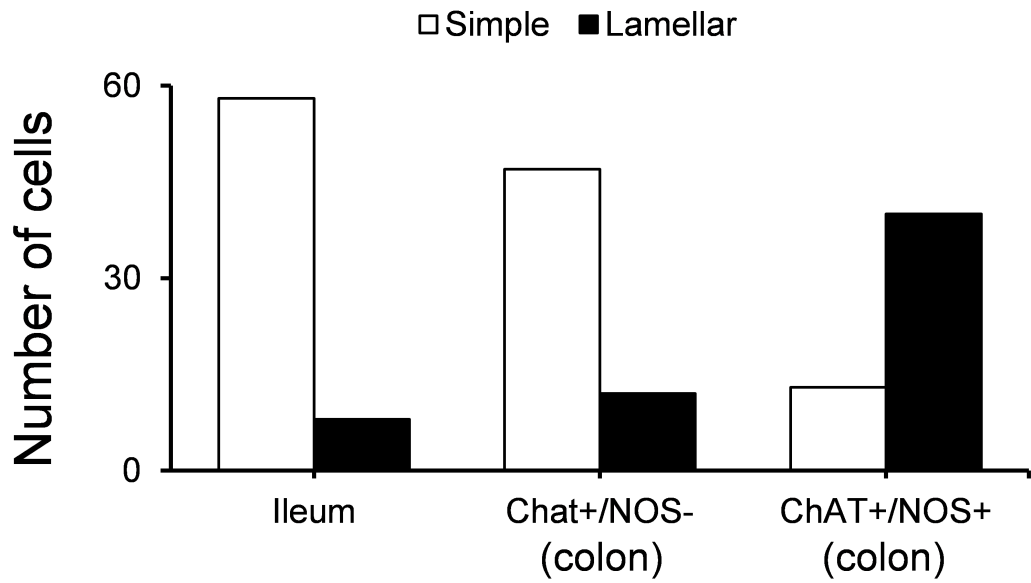


Figure 5.16

Biotinamide labelled cell bodies of viscerofugal neurons in guinea pig ileum. The majority of viscerofugal neurons in the ileum had small nerve cell bodies with a simple morphology. (A-J) Examples of viscerofugal neurons with simple cell morphology. (K-M) Viscerofugal neurons with lamellar morphology; these were a small minority (12%) in the small intestine.

A Morphology of viscerofugal neurons



B

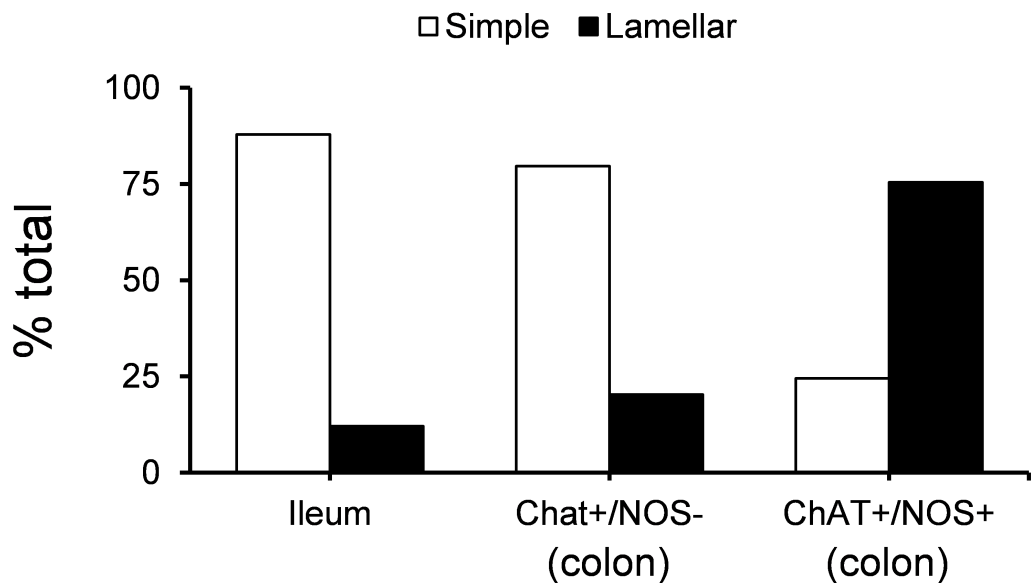


Figure 5.17

(A) The occurrence of simple morphology (white bars) and lamellar morphology (black bars) among viscerofugal neurons in the ileum, compared with the colon. Viscerofugal neurons in the ileum mostly had simple cell body morphology. (B) Viscerofugal neuron cell body morphology expressed as proportions. Similar proportions of simple and lamellar cell body morphologies occurred in viscerofugal neurons in the ileum and in colonic ChAT+/NOS- viscerofugal neurons.

The distribution of viscerofugal nerve cell body sizes in the ileum and colon

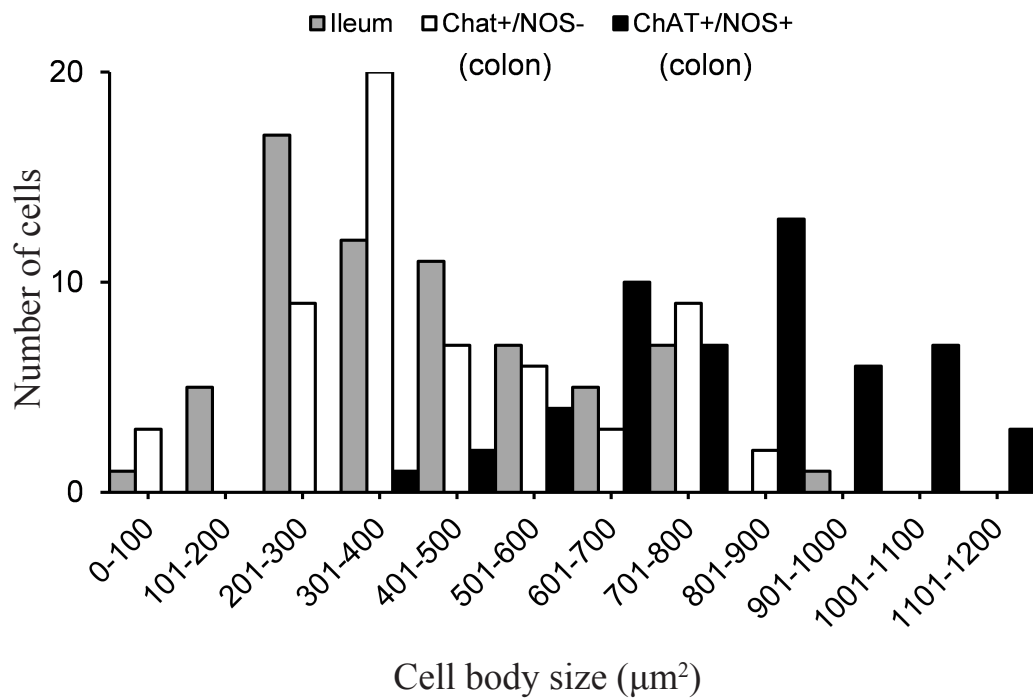


Figure 5.18

A frequency histogram of the sizes of viscerofugal neuron cell bodies in ileum, compared with the major populations of the colon. Viscerofugal nerve cell bodies in the ileum were not significantly different in size to ChAT+/NOS- viscerofugal neurons in colon (most of which had simple morphology). However, they were significantly smaller than colonic ChAT+/NOS+ viscerofugal neurons, which had predominantly lamellar soma-dendritic morphology.

The spatial distribution of viscerofugal nerve cell bodies labelled from mesenteric nerves in the ileum

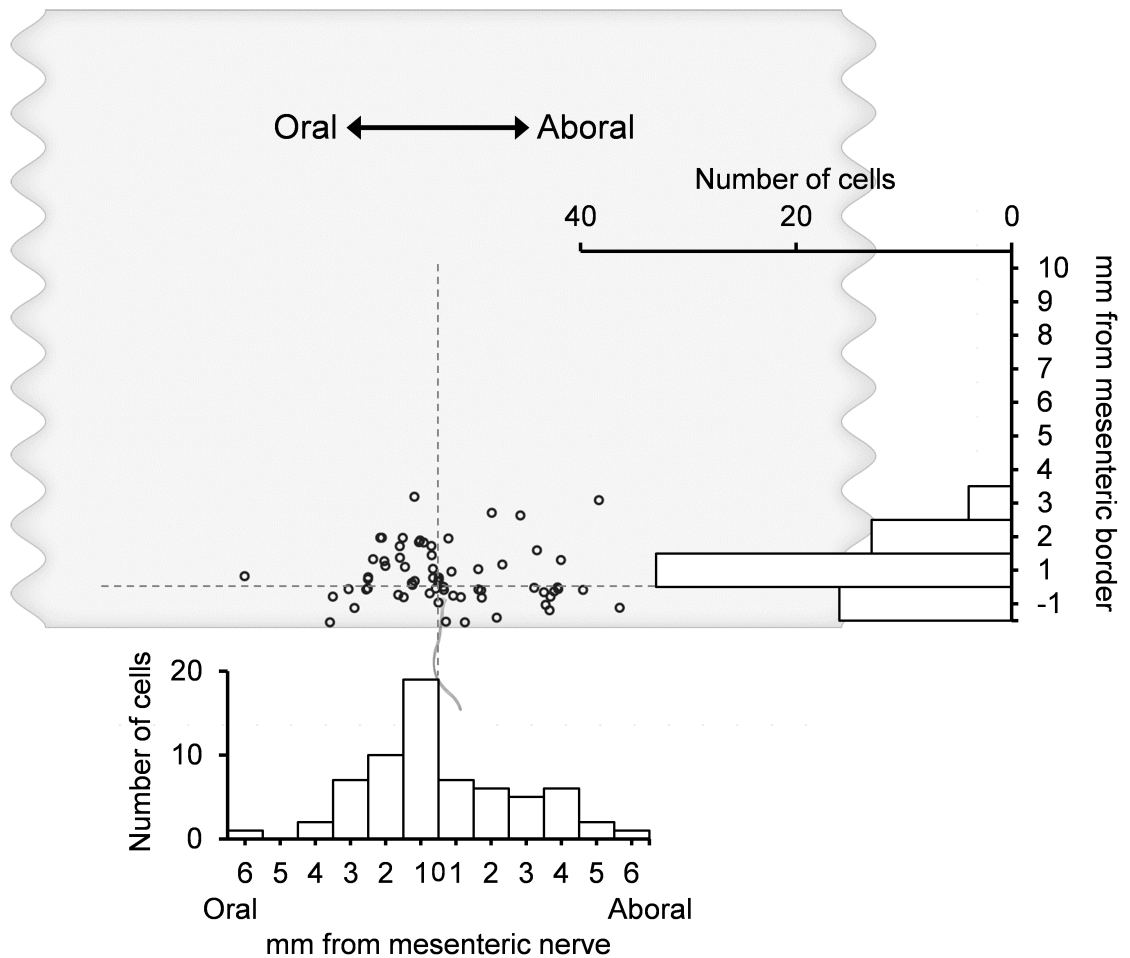


Figure 5.19

The spatial distribution of viscerofugal nerve cell bodies in the ileum. This figure shows the locations of 66 viscerofugal neurons labelled from mesenteric nerve trunks (15 preparations, $n=13$). Frequency histograms of their circumferential and longitudinal distributions are shown adjacent and below the composite map, respectively. The nerve cell bodies of viscerofugal neurons in the ileum were tightly clustered near the mesenteric border circumferentially, similar to colonic ChAT+/NOS- viscerofugal neurons. However, unlike those in the colon, viscerofugal nerve cell bodies in the ileum were distributed normally about the mesenteric nerve entry with an oral or aboral bias. In this figure, the dashed lines indicate the point of entry of the mesenteric nerve into the myenteric plexus, in both axes.

DISCUSSION

In this study, we calculated that 38% of viscerofugal neurons expressed both ChAT and NOS in their cell bodies. ChAT and NOS alone were expressed in 44% and 11% of cell bodies, and 7% of cell bodies did not express either ChAT or NOS. The populations of ChAT+/NOS- and ChAT+/NOS+ neurons were identified previously (Anderson et al., 1995, Mann et al., 1995). The presence of NOS in viscerofugal neurons may reflect region-specific variation in chemical coding – known to occur among other classes of enteric neurons (Messenger and Furness, 1990, Anderson et al., 1995). Alternatively, the presence of NOS in viscerofugal neurons may represent functional differentiation. In the present study we additionally showed that ChAT+/NOS+ viscerofugal neurons are differentiated from ChAT+/NOS- viscerofugal neurons not only by their neurochemical content, but also by their cell body morphology, and in their spatial distributions in the gut wall in both circumferential and longitudinal axes.

Viscerofugal neurons that contained NOS had larger cell bodies than neurons that lacked NOS, as well as lamellar dendrites and tended to descend along the gut before exiting via extrinsic nerves. Conversely, viscerofugal neurons that lacked NOS had small and simple cell body morphologies, and tended to ascend before exiting the gut. NOS catalyses nitric oxide synthesis, a diffusible gas that activates soluble guanylyl cyclase or nitrosylates cysteine residues (Ahern et al., 2002). In the gut, nitric oxide is prominently involved in inhibitory neuromuscular transmission (Rivera et al., 2011), and in neuron-to-neuron transmission (Dickson et al., 2007, Bornstein et al., 2010). In addition to viscerofugal neurons, NOS is present within

descending interneurons and inhibitory motor neurons (Lomax and Furness, 2000). The relationship observed in the present study between NOS content, axonal projections, and cell morphology in viscerofugal neurons parallels the characteristics of other NOS-containing enteric neurons. Lesion studies in colon suggest all myenteric neurons containing NOS have descending projections (McConalogue and Furness, 1993). Descending enteric neurons containing NOS were also primarily Dogiel type I lamellar neurons (McConalogue and Furness, 1993), consistent with NOS-containing viscerofugal neurons in the present study. In addition, descending NOS-immunoreactive inhibitory motor neurons and interneurons have larger cell bodies and dendrites than excitatory motor neurons and ascending interneurons, which lack NOS (Brookes et al., 1991b, Schemann and Schaaf, 1995, Brookes et al., 1998). Thus, these common morphological features among enteric neurons with similar neurochemical phenotypes, occurs across functional classes. It is possible that common mechanisms may affect axonal growth among enteric neurons with similar neurochemical phenotypes, regardless of function. Exactly how NOS and enteric neuronal morphology are linked is not clear. However, a direct relationship between nitric oxide signalling and neuronal morphogenesis have recently been identified in other species and neuronal systems (Bradley et al., 2010, Cooke et al., 2013).

The observed morphological differences between the ChAT+/NOS+ and ChAT+/NOS- populations of viscerofugal neurons in the colon raise the possibility of functional differences. If cell surface area is associated with the number of presynaptic inputs on enteric neurons, as reported in other autonomic neurons (Purves et al., 1988), it is possible that ChAT+/NOS+ viscerofugal neurons integrate more synaptic inputs than ChAT+/NOS- neurons. In addition, the differences in cell

body size among viscerofugal neurons are likely to confer differences in cell capacitance, input resistance and time constant. These possibilities require direct confirmation. The implication of different circumferential distributions among populations of viscerofugal neurons is not clear, as there is little available data on how enteric neural circuits are distributed around the circumference of the gut.

In this study we analysed the cell bodies of every biotinamide labelled viscerofugal neuron in all preparations, amounting to 137 neurons. Of these, 57 had a single visually discriminable axon emerging from their cell body. Axons in the remaining 80 viscerofugal neurons could not be confidently discriminated from surrounding biotinamide-labelled extrinsic nerve fibres. In a previous retrograde labelling study, multipolar viscerofugal neurons have been identified (Ermilov et al., 2003). It is possible there were multipolar viscerofugal neurons among the 80 neurons in the present study whose axons could not be confidently discriminated. However, in the accumulated retrograde labelling studies of several hundred viscerofugal neurons, we have identified multipolar viscerofugal neurons rarely (accounting for less than 1% - see **chapter 6, figure 6.08** and **6.09** for examples of these). Thus, the finding that none of 57 viscerofugal neurons in the present study were multipolar is consistent with these findings.

Two populations of viscerofugal neurons identified in the present study that lack immunoreactivity for ChAT have not been identified previously in retrograde tracing studies. All NOS⁺ and ChAT⁺ cell bodies, labelled with and without biotinamide, were easily detected above background labelling; therefore, it seems unlikely that our observations are solely due to the inability of antisera against these enzymes to detect

antigen presence in unlabelled cell bodies. As stated above, previous examinations of viscerofugal neuron immunohistochemistry in the distal colon accounted specifically for populations targeting the coeliac and inferior mesenteric ganglia. The hitherto unidentified populations of ChAT-/NOS+ and ChAT-/NOS- viscerofugal neurons may therefore project to other targets, such as the superior mesenteric ganglion (Messenger and Furness, 1993), pelvic ganglia (Luckensmeyer and Keast, 1995a), or spinal cord (Neuhuber et al., 1993, Suckow and Caudle, 2008). The absence of ChAT-immunoreactivity from 21% of colonic viscerofugal cell bodies challenges the assumption that all cells in this population are cholinergic.

In summary, we have retrogradely traced viscerofugal neurons from extrinsic nerve trunks into the gut. Their cell bodies were tested for immunoreactivity to the neurotransmitter-synthesizing enzymes choline acetyltransferase and nitric oxide synthase, revealing four chemically coded populations: ChAT+/NOS-; ChAT+/NOS+; ChAT-/NOS+ and ChAT-/NOS- viscerofugal neurons. The latter two groups have not previously been identified and may represent non-cholinergic populations. The previously identified populations of ChAT+/NOS- and ChAT+/NOS+ viscerofugal neurons were further distinguished neurochemically, morphologically and spatially, suggesting they may represent functional subclasses of viscerofugal neurons.